# Efficient Automatic Oriented Lung Boundary detection and Screening of Tuberculosis using Chest Radiographs

Rema Devi.V
University College of Engineering, Konam, Nagercoil, India.

Viveka.T
University College of Engineering, Konam, Nagercoil, India

**Abstract – The main objective is the accurate detection of the lung boundary and tuberculosis screening using chest Radiographs. In existing system different methods are specified like rule based methods, pixel classification methods and deformable model based methods. These methods have mostly heuristic assumptions and it provides only approximate solutions. In proposed method a robust lung segmentation system is introduced for chest X-ray images. Non-rigid registration-driven robust lung segmentation method using following methods. The method consists of three main stages: 1) first a content-based image retrieval approach for identifying training images and shape similarity measure with GLCM Metrics to measure matrix of frequencies at which pixels . Separated by a certain vector and intensity of a pixel in position of images, then creating the initial patient-specific anatomical model of lung shape using SIFT-flow for deformable registration of training masks to the patient CXR. Extracting refined lung boundaries using a level set optimization approach with a customized energy function.**

**Index Terms – Chest X-ray imaging, computer-aided detection, Image registration, image segmentation, tuberculosis (TB).**

## 1. INTRODUCTION

Detecting the lung regions in chest X-ray images is an important component in computer-aided diagnosis (CAD) of lung health. In certain diagnostic conditions the relevant image-based information can be extracted directly from the lung boundaries without further analysis. For example, shape irregularity, size measurements, and total lung volume provide clues for serious diseases such as cardiomegaly, pneumothorax, pneumoconiosis, or emphysema. In the case of CAD-based identification of lung diseases, accurate lung boundary segmentation plays an important role in the subsequent stages of automated diagnosis. This system is being developed as part of a project aimed at screening of tuberculosis (TB) patients in regions of the world with high incidence of disease but inadequate healthcare facilities. The initial screening region will be rural areas of western Kenya, using light weight portable X-ray scanners. The shortage of radiological infrastructure and radiologists in rural areas of Kenya necessitates an automated TB screening approach in such resource constrained regions. One of the important steps in automatic analysis of chest X-ray images is to detect the lung boundaries accurately. There are a number of anatomical challenges and subtle cues involved in segmenting the lung region within a CXR. In this paper, we present a lung boundary detection system incorporating non-rigid registration with a CXR database of presegmented lung regions to build an anatomical atlas as a guide combined with graph cuts based image region refinement. The initial work is significantly expanded in this paper to incorporate a deformable anatomical lung model using a novel non-rigid registration approach based on SIFT-flow, a detailed assessment of the approach compared to other state-of-the-art methods using the validated Japanese Society of Radiological Technology (JSRT) dataset and further experimental validation of the approach using two additional CXR databases.

## 2. PATIENT- SPECIFIC STATISTICAL LUNG ATLAS MODEL USING NONRIGID REGISTRATION

Segmentation in medical imaging poses a number of challenges including multiplicative noise, motion during imaging, sampling artifacts caused by the acquisition equipment, low contrast, deformation of tissues and anatomical shape variations due to normal anatomy and disease. Therefore, classical segmentation techniques, which make simplifying assumptions of rigid motion or additive noise for example, and do not use *a priori* information, usually produce unsatisfactory results on medical images. In order to provide *a priori* information for improved segmentation, we incorporate a lung atlas model into the system. Since the X-ray images contain variable lung shapes, a static model is not sufficient to describe the lung regions. Our system therefore estimates a statistical model for each patient X-ray using a training set of segmented images

(atlases) to identify the most similar images followed by a non-rigid registration algorithm to warp the most similar training masks to the patient CXR.

- CBIR Paradigm for Inter-Patient Matching
- SIFT-Flow Deformable Warping of Lung Atlas

### 2.1. CBIR Paradigm for Inter-Patient Matching

We first identify a small subset of images (i.e., five) in the training database that are most similar to the patient query image, using a content-based image retrieval (CBIR) inspired approach, and use this subset of training images including corresponding lung masks to develop a patient-specific lung model. Using a small subset of images from the database is sufficient to build an accurate lung model while significantly speeding up the step of non-rigid registration between the training and the patient query images. Ranking precedes registration, otherwise we would need to extract SIFT features and compute SIFT-flow deformable registration models for every image in an extensive training database which is prohibitively expensive and impractical for a fieldable system. Unlike other patient-specific lung models in the literature that use intra patient image information , we develop an interpatient matching and image retrieval system that follows the CBIR paradigm to guide segmentation. CBIR systems are designed to be fast for online retrieval applications with an offline preprocessing step to extract signature features for each image in the database and can incorporate multimodal information to improve precision.

CBIR systems usually produce a ranked subset of images most similar to the query which in our case is a new patient CXR image. We assume that the CXR database has been appropriately preprocessed and consists of globally aligned and normalized CXRs. We use *partial* Radon transforms, or orthogonal projection profiles, to compare and rank the similarity between two patient's lung images. The Radon transform projection along an arbitrary line in the - plane is defined as

$$R(\rho,\theta) = \iint I(x,y)\delta(\rho - x\cos\theta - y\sin\theta)dxdy \quad (1)$$

Where is the 2-D impulse function

$$\iint_{-\infty}^{\infty} \delta(x,y)dxdy - 1 \quad (2)$$

And has the shifting property

$$\iint_{-\infty}^{\infty} I(x,y)\delta(x - x_{0,}\, y - y_0)dxdy = I(x_0,y_0) \quad (3)$$

With

$$\delta(x,y) = \begin{cases} \infty, & if\ x = y = 0 \\ 0, & otherwise \end{cases} \quad (4)$$

The partial Radon transform projection method is fast to compute and only an approximate matching atlas set of lung segmentations from the CXR database is needed to compute a spatial prior that can be refined in the subsequent phase of the algorithm. Our X-ray sets contain only a small number of slightly rotated images. The Spatial Filter process in TNTmips (Image / Filter / Spatial Filter) includes a set of Gray Level Co-occurrence Matrix filters designed to extract information about the texture of an image. For a grayscale image (or component of a color image), image texture is defined by the amount, spatial scale, and spatial pattern of variation in brightness values. Some areas of a grayscale image may show little variation in brightness (gray level) over large areas; these areas appear visually smooth. Other image areas may show many large changes in gray level over short distances, and appear visually rough. Texture can be used along with other characteristics in image classification operations. Gray Level Co-occurrence Matrix (GLCM) filters operate by computing, for each filter window position, how often specific pairs of image cell values occur in neighboring cell positions (such as one cell to the right). The results are tabulated in a co-occurrence matrix, and specific statistical measures are computed from this matrix to produce the filtered value for the target cell. The registration performance is significantly improved when a personalized lung model is designed by comparing the patient X ray with presegmented lung images in the Fig. 3. Plots show the Radon transform profiles for a query and database image, for, left image, and, for the right image. CXR database using a fast shape similarity measure based on partial Radon transforms.

### 2.2. SIFT-Flow Deformable Warping of Lung Atlas

Image registration is an important task for many medical applications such as comparing/fusing images from different modalities, tracking temporal changes in medical images collected at different times. A registration scheme calculates a transformation mapping from source image to target image by matching corresponding pixels of images. Correspondences can be calculated either for each pixel or only for salient locations such as edge points or corners. Should be modelled efficiently. The SIFT-flow algorithm models local gradient information of the observed image using the Scale Invariant Feature Transform (SIFT). The SIFT features of the X-rays are calculated as follows. First, the gradient orientations and magnitudes are computed at each pixel. The gradients are weighted by a Gaussian pyramid in a region (e.g.,) in order to increase the influence of the gradient in the center. Then, the regions are subdivided into (e.g.,) quadrants. In each quadrant, a gradient orientation histogram is formed by adding the gradient values to one of eight orientation histogram bins. The concatenation of orientation histograms of the quadrants form

the SIFT descriptor vector for the center pixel of the region. Once we have calculated the SIFT features for the image pair, the registration algorithm computes pixel-to-pixel correspondences by matching the SIFT descriptors. The correspondence matching is formulated using the following objective function:

$$\mathrm{E(w)} = \sum_{p \in P} \min(||S_1(p) - S_2(p + w(p)||, t) + \sum_{p} (\mathrm{u|p|} + \mathrm{v|p|})) + \sum_{(p,q) \in N} \min(|u(p) - u(q)|, d) + \min(|v(p) - v(q)|, d)) \quad (6)$$

Where is the set of pixels in the X-ray; is the spatial neighborhood set, and are the SIFT images in which each pixel is represented by a SIFT descriptor vector; are the flow vectors at and are the truncated thresholds. The minimization algorithm calculates the SIFT-flow by minimizing the objective function. The first term of the objective function forces the algorithm to match pixels according to their SIFT descriptors, with warping based on the registration flow vector. The second term constrains the flow vectors to be as small as possible.

The third term constrains the flow vectors of neighboring pixels to be similar. The registration algorithm that we employed applies the transformation mapping for each pixel independently. Therefore, the registered masks forming the lung atlas model have rough boundaries. We use cubic spline interpolation to obtain smoother boundaries of the lung masks.

In order to preserve the important regions of the lung boundary such as cost phrenic angle regions, instead of equal sampling, we extract the critical points
Some of them focused on registering different views of the same scene in which a relatively simple transformation will be sufficient for registration.

In our case, in order to create a lung model, we register chest X-rays from different patients of the contour by using the computed patient specific lung model is a probabilistic shape prior in which each pixel value is the probability of the pixel being part of the lung field.

$$\mathrm{K}(s_1, s_2) = \frac{|\theta(s_1, s_2) - 180| l(s_1) l(s_2)}{l(s_1) + l(s_2)} \quad (7)$$

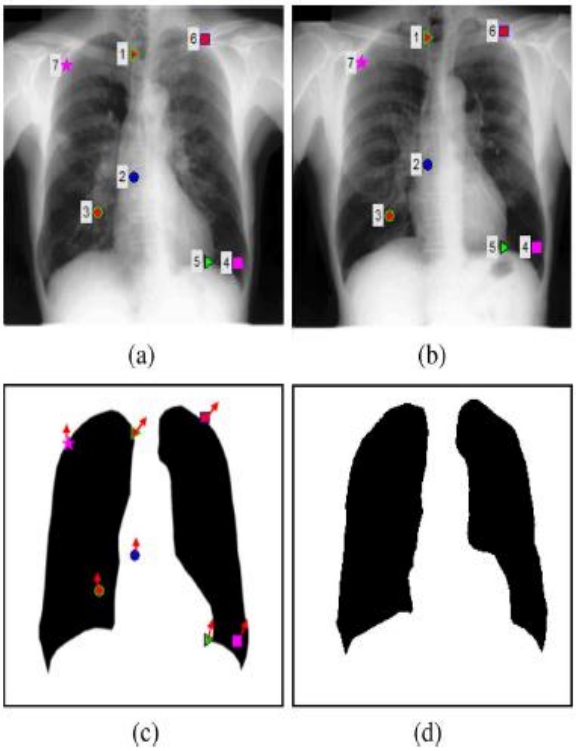


Figure. 2 illustrates the registration stage of the proposed system.

Fig. 2(b) is the patient X-ray. Fig. 2(a) is the most similar X-ray to the patient X-ray in the database chosen according to the shape similarity between the lungs. The SIFT-flow algorithm calculates corresponding matches for each pixel of these X-ray pair by solving the flow vectors. Colored markers indicate corresponding matches for a few pixel samples. We see that the lung boundary in one X-ray image approximately matches the lung boundary in the other X-ray. The spatial shifts between corresponding matches define the transformation mapping for pixels. The algorithm applies the transformation mapping by simply shifting each pixel in the training mask according to the calculated shift distance [Fig. 2(c)]. The registered mask is shown in Fig. 2(d). The registration stage is repeated for each of the top- (e.g.,) similar X-rays to the patient X-ray. The lung model for the patient X-ray is built-up using the mean of the top-ranked probability of the pixel being part of the lung field. Where denotes the line segment between and denotes the line segment between and is the outer turn angle between and are the length of and, respectively. This measure aims to remove points with short and straight neighboring line segments. The iteration is terminated when the number of critical points reaches a prespecified value.

## 3. PORPOSED MODELLING

The system detects the lung boundary of X-ray images using image properties and the lung model calculated in the previous stage. We perform image segmentation using level set formulation the active contour is a oving front denoted by *C* which is represented implicitly by the zero level set $C(t) = f(\sim x)jÁ(t; \sim x) = 0g$ of a level set function $Á(t; \sim x)$. The proposed adaptive stopping force which allows the contour to bridge the invalid features and stop only at the valid ones. Our approach builds on the work of that proposed a robust parametric active contour able to discard outlier features. The features used are connected sets of edge points, called strokes, which are more reliable than edge points.

### 3.1 Contour initialization

The contour is automatically initialized at the outer chest wall, by a very simple yet effective method. The binary image obtained by gray-level thresholding using Otsu's method that was used to detect edges is processed by a morphological flood filling operation to remove wholes. Then, the region with the largest area is retained and the initial contour is placed around this region. Furthermore, the edges outside this region are removed to prevent them from attracting the contour.

The features used are connected sets of edge points, called strokes, which are more reliable than edge points.

We will start by introducing some notation. Let *y* be the set of all edge points detected in an image and let us assume that *y* is organized in connected components, called strokes, $y_j ; j = 1; :::;N$ where $y_j = fy_{j\ 1}; :::; y_{jn}\ g$ is the set of edge points belonging to the j-th stroke. A standard edge linking algorithm is used to compute the image strokes.

The automatic segmentation of the lungs in X-ray computed tomography (CT) images using level set segmentation. Level set methods usually produce over segmented images of the lungs due to the presence of outliers features.

(a)

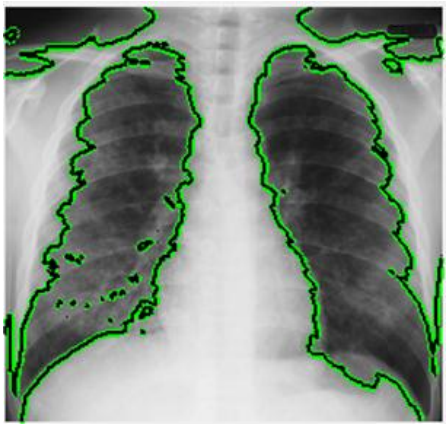

(b)

Figure. 3 illustrates the registration and segmentation stage of the proposed system.
Fig. 3(a) is contour image registration stage. Fig. 3(b) is the patient X-ray's detected image.

## 4. RESULTS AND DISCUSSIONS

In this section all the results and the discussions should be made.

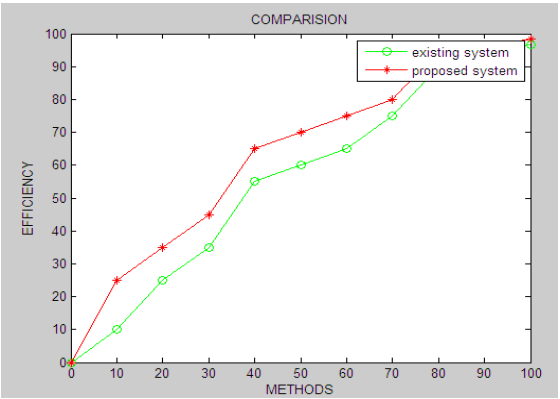


Figure 1 Resultant Graph of the Proposed System

## 5. CONCLUSION

We have presented a robust lung boundary detection method that is based on a patient-specific lung atlas using fast partial Radon profile similarity selection and SIFT-flow non-rigid registration with refinement using a level set segmentation algorithm. We evaluated the algorithm using three different datasets containing 585 chest radiographs from patients with normal lungs and various pulmonary diseases. On the publicly available JSRT dataset, experimental results showed an accuracy of 95.4% (overlap measure), compared to the expert segmentation gold standard, which is the highest machine performance reported in the literature. On the other CXR datasets from Montgomery County and India, with more

challenging pathologies including abnormal lung boundaries, the same algorithm shows consistently high detection accuracies of 94.1% and 91.7%, respectively. These are the first results reported for automatic lung boundary segmentation that include abnormal lung shapes. The results indicate the robustness and effectiveness of the proposed approach when applied to CXRs collected in different geographical regions. A point to note here is that fluid-filled lungs are radio-opaque, and any radiologist-marked "ground-truth" lung boundary is only an estimate.

## REFERENCES

[1] Tony F.Chan, Luminita A. Vese, "Active Contours Without Edges,"IEEE Trans. Med. Imag., vol. 10, no. 2, Feb. 2001.
[2] J. Paul, M. Levine, R. Fraser, and C. Laszlo, "The measurement of total lung capacity based on a computer analysis of anterior and lateral radiographic chest images," IEEE Trans. Biomed. Eng., vol. 21,no.6,pp.444–451,Nov.1974.
[3] Bino Sebastian V,Unnikrishnan A and Kannan Balakrishnan,"Gray Level Co-Occurrence Matrices:Generalization and some new features", Signal & Image Processing : An International Journal Vol.2, No.2, April 2012.
[4] H. Becker, W. Nettleton, P. Meyers, J. Sweeney, and C. Nice, "Digital computer determination of a medical diagnostic index directlyfrom chest X-ray images," IEEE Trans. Biomed. Eng., vol. 11,pp.67–72,1964.
[5] Mari Partio,Bogdan Cramariuc,Moncef Gabbouj and Ari Visa,"Rock Texture Retrieval Using Gray Level Co-Occurrence Matrix", June 6, 2001.
[6] T. F. Cootes, C. J. Taylor, D. H. Cooper, and J. Graham, "Active shape models—Their training and application,"Comput. Vis. Image Understand., vol. 61, no. 1, pp. 38–59, 1995.
[7] B.Ginneken,A.F.Frangi,J.J.Staal,B.M.Romeny,andM.A. Viergever, "Active shape model segmentation with optimal features," IEEE Trans. Med. Imag., vol. 21, no. 8, pp. 924–933, Aug. 2002.
[8] M. Rahman, S. Antani, D. Fushman, and G. Thoma, "Biomedical image retrieval using multimodal context and concept feature spaces," Med. Content-Based Retrieval Clin. Decision Support, vol. 7075, pp. 24–35, 2012.
[9] L. Hogeweg, C. Snchez, P. A. Jong, P. Maduskar, and B. Ginneken, "Clavicle segmentation in chest radiographs,"Med. Image Anal., vol. 16, no. 8, pp. 1490–1502, 2012.
[10] T. Yu, J. Luo, and N. Ahuja, "Shape regularized active contour using iterative global search and local optimization," inProc. IEEE Comput. Soc. Conf. Comput. Vis. Pattern Recognit., 2005, vol. 2, pp. 655–662.

Authors

**Rema Devi.V** is currently a student of University College of Engineering,Nagercoil Campus in the Department of Computer Science and Engineering, She graduated in Computer Science & Engineering from Anna University, Chennai.

**Viveka T** is currently a Teaching Fellow in the Department of Computer Science and Engineering,University College of Engineering,Nagercoil Campus. She graduated in Computer Science & Engineering from Anna University, Chennai and did her master's degree in Computer Science & Engineering.